INTERNATIONAL JOURNAL OF PRECISION ENGINEERING AND MANUFACTURING Vol. 17, No. 11, pp. 1503-1514 NOVEMBER 2016 / 1503
DOI: 10.1007/s12541-016-0176-8 ISSN 2234-7593 (Print) / ISSN 2005-4602 (Online)

Experimental Study of Cooling Speed for Ultra-Thick Steel Plate during the Jet Impinging and Quenching Process

Tian-Liang Fu[1,#], Xiang-Tao Deng[1], Guo-Huai Liu[1], Zhao-Dong Wang[1,#], and Guo-Dong Wang[1]

1 The State Key Lab of Rolling and Automation, Northeastern University, No.11, Lane 3, Wenhua Road, Heping District, Shenyang, 110819, Liaoning Province, China
Corresponding Author / E-mail: futianliang@126.com, TEL: +86-13998836391, FAX: +86-024-23906472
E-mail: 35741193@qq.com, TEL: +86-13904006426, FAX: +86-024-23906472

KEYWORDS: Ultra-thick steel plate, Jet impingement and quench, Heat transfer mathematical model, Cooling speed, Temperature gradient

The quenching temperature drop curve for Q345B steel plate with 84 mm and 170 mm thickness was tested to analyze the distributing regularities and influencing factors of cooling speed for ultra-thick steel plate during the jet impinging and quenching process. The influences for temperature drop, temperature gradient and cooling speed were analyzed under the conditions of 60~100 m^3/h water amount, 0.4~1.0 MPa water pressure, transient switching of quenching mode and the distribution of heat exchanger. Three-dimensional heat anti transfer model, surface heat transfer coefficient model and thermal physical parameter model were built up by finite element and optimization. The results showed that the deviation of calculated and measured values was less than 4% for temperature drop curve model. The cooling speed of vertical section for 84 mm-thick steel plate was approximately proportional to surface heat transfer coefficient. The influence of surface heat transfer to cooling speed became weak when the thickness was increased. The influences of temperature effect when switching different quenching modes and temperature gradient of vertical section to cooling speed were stronger. The minimum value of cooling speed was about 1.0~1.8°C/s, between H/6 and H/3 region. These data provide the key information for increasing the cooling speed and uniformity.

Manuscript received: December 8, 2015 / Revised: May 31, 2016 / Accepted: June 30, 2016

NOMENCLATURE

Ac_1 = Formation temperature of tested steel austenitic
Ac_3 = Complete transition temperature of tested steel austenitic
A_m = Heat conductivity matrix
Ar_1 = Decomposition temperature of tested steel austenitic
Ar_3 = Precipitation temperature of tested steel ferrite
B = Width of steel plate
B_m = Heat capacity matrix
Ceq = Carbon equivalent of tested plate
$c(T)$ = Specific heat function of steel plate
C_V = Heat load vector
F_i = Cubic shape functions of serendipity family
F_N = The number of functions being formed, in this paper $F_N = 64$
$f(p_i)$ = Objective function defined by formula 1
G_i = Cubic spline function
H = Thickness of steel plate
H_i = Hermitian shape function
$h(y,z,\tau)$ = Surface heat transfer coefficient of steel plate
K_T = Time cycles
L = Length of steel plate
M_s = Martensitic transformation start temperature of tested steel
M_f = Martensitic transformation finish temperature of tested steel
N_p = Number of temperatures being recorded by one temperature measuring point
N_t = Number of temperature measuring points
P_i = Variable function of heat transfer coefficient for joint element in unit time
p_i = Minimized parameter
$q^g(x,y,z)$ = Research on heat flux density of steel plate in a plane
S_e = Scope of cell surface
S_s = State of boundary condition, if the known $S_s = 1$, or else $S_s = 0$
T = Three dimensional temperature field of steel plate
$T^m{}_n$ = Calculated temperature at τ_n of temperature measuring point
$Te^m{}_n$ = Measured temperature at τ_n of temperature measuring point
T_m = The unknown temperature at element joint

T_s = Surface temperature of steel plate
T_w = Temperature of water
V = Scope of cubic element
v_J = Jet impinging speed
v_N = Jetting speed of circular orifice
W_j = Quadratic spline function
x,y,z = Cartesian coordinate

GREEK SYMBOLS

$\varepsilon = \varepsilon = 1\ e^{-10}$ Minimum value determined norms
ξ_1, ξ_2, ξ_3 = Natural coordinate of cubic unit
η_x, η_y, η_z = Natural coordinate of Hermitain interpolating shape function
$\lambda(T)$ = Heat conductive coefficient function of steel plate
$\rho(T)$ = Density function of steel plate
ρ_w = Water current density in jet impact zone
τ = Time
ΔD_{ave} = Average derivative of objective function
ΔT_{ave} = The measured and calculated average temperature deviation
Φ = Initial temperature field of steel plate

1. Introduction

Water jet impingement cooling is different from the other heat transfer method, as it can achieve the larger convective heat flux when the wall superheat is relatively high and the heat flux changing is obvious with the small changes of wall temperature.[1] Therefore, ultra-thick steel plate (≥ 80 mm) can be quenched by water jet impingement cooling method after being rolled. Steel structure is regulated by controlling the cooling speed and cooling uniformity of the section which can improve the performance of strength and toughness.[2,3] Steel plate is needed to be heated to 900~1000°C before quenching. The process of jet impinging and quenching contains various forms, such as internal three-dimensional heat conduction, jet impinging heat transfer in stagnation region, nucleate and transition boiling heat transfer, film boiling heat transfer, radiant heat transfer and so on. Single-phase forced convection and boiling heat are coupled with each other. The heat transfer is a very complicated process.[4] In addition, heat transfer of steel plate surface is related with various factors, such as jetting speed, jetting diameter, jetting angle, super-cooling degree, and wall superheat, which further increase the controlling difficulty of internal temperature field and cooling speed.[5] Thus, it is necessary to study how jetting parameters affect the surface heat transfer and internal heat conduction, what is the developing regularity and influencing factors of cooling speed, which are important for the prediction of quenching technic parameters and performance optimization for ultra-thick steel plate.

Currently, the experimental researches of jet impinging and quenching process for high temperature steel plate are limited in transient or steady state. Most of them focus on the relationships between surface heat flux density, heat transfer coefficient, critical heat flux density value and injection parameters for different nozzle types,[6] jetting angle,[7] jetting length,[8] jetting speed, super-cooling degree, initial temperature, physical property parameters, for thin steel plate (≤ 25 mm). Wall Nu number distribution is tested under low Re number condition (Re ≤ 20000), and the numerical model is also be constructed.[9-11] The transient cooling and boiling curves were studied when jetting the surface of steel plate with round hole.[12] The plate size was 2 mm 50~210 mm^2 and the testing parameters like heating temperature was 1100°C, super-cooling degree was 5~80°C and jetting speed was 2~7 m/s. The changing of transient temperature near surface was tested using thermocouples. Meanwhile, the heat flux density and the surface temperature were calculated later.Similar characteristics of boiling curves were obtained in other researches.[13] Temperature control system which could measure 700°C surface temperature was designed to test the whole local boiling curve under steady-state condition.[14] The results indicated that super-cooling degree and jetting speed had little influence to heat flux density but greater influence to CHF value. Similar results were gained when the influences of jetting speed (1~3.17 m/s) and super-cooling degree (5~55°C) to water cooling and boiling curves at jetting stagnation point were studied as the upper surface temperature limit was 1027°C.[14,15] Using rotating cylinder jetting to impinge the water-cooling device which simulated the moving-cooling process of steel plate after hot rolling, cooling and boiling curves were tested under the conditions of 500~600°C initial temperature, 10~83°C super-cooling degree and 0.8~1.2 m/s jetting speed.[16] The results showed that super-cooling degree had obvious effects on CHF value which was consistent with the previous studies.[6,14] Theoretical and experimental researches about boling and heat transfer were carried out when jetting high temperature flat membrane with round hole.[17] Compared with jetting speed, super-cooling degree had greater influence to heat flux density at Leidenfrost point and film boiling area. Mechanisms of boling and heat transfer at jetting stagnation point were studied for 2 mm × 300 mm^2 steel plate during jetting and cooling process.[18] The distribution of heat flux density at heat transfer zone, as well as the boling curve at 15.3 m/s jetting, 85°C super-cooling degree and 827°C wall superheat, were given out.

Valuable achievements were gained when the relationship between surface heat transfer and internal heat conduction of steel plate was revealed, and the heat transfer model for temperature field was constructed. One dimensional inverse heat conduction method (IHCM) was used to calculate heat flux density and heat transfer coefficients, with 1.1 mm thickness the alloy plate as material, steam fog cooled after being heated to 300°C.[19] The influences of cooling parameters to heat transfer coefficients or heat flux density were studied by inverse heat conduction method during the process of heat treating.[20,21] However, problems of convergence and uniqueness of solution appeared when inverse heat conduction method was used.[22,23] Regularization method was proposed to solve this kind of problem, although it had the limitation that regularized item might influence the precision of solution.[22,24] Temperature field analysis method gradually turned into the problem of three-dimensional inverse heat conduction with the development of heat transfer technology. Three-dimensional analytic method which could simulate temperature sensor to test values was first proposed with CFX4.2 co mmercial software.[25] Similar temperature simulation methods were reported and showed that temperature field simulation converged more easily only when target function was

established with large amount of temperature measurements.[26,27] Numerical methods like finite difference method, finite element method and finite volume method were widely used to analyze internal temperature field of steel plate. Local jet impact heat transfer coefficient of steel plate surface with high temperature and temperature gradient were calculated by heat transfer equation from two-dimensional finite difference model using 25 mm × 200 mm × 410 mm steel plate, 900°C heating temperature, and 15~35 L/min recycled water volume.[1] Based on nonlinear function, three-dimensional finite element model was used to analyze heat conduction problems of EN1.4724 steel plate during jetting and cooling process with only 2°C model calculation deviation.[28] The size of steel plate was 8 mm × 90 mm × 100 mm. Heat cooling-transfer and phase transfer model was exploited to calculate the temperature of strip steel and phase volume fraction after hot rolling of strip steel with consideration of influence from phase transformation latent heat.[29]

Taken together, the current researches of high temperature plate heat transfer during quenching process mainly focused on sheet steel plate (H ≤ 25 mm) with unchanged jetting parameters which was not consistent with the goal to control the section temperature gradient and cooling speed according to the technological path for ultra-thick steel plate (H ≥ 80 mm).To achieve this goal, two experimental problems are needed to be solved. First, in order to reduce the influence of lateral temperature dropping to temperature field, the width and length of plate should be much larger than thickness. Therefore, quenching device with large enough size, recycled water volume and jetting pressure are needed to be designed to achieve continuously adjustable jetting parameters and match with high-power heating furnace and crown block; Second, measurement of micro heater array, cooling of thin foil and temperature oscillation IR thermography were not applicable as the initial wall temperature was higher than 900°C and duration of the quenching was more than 10 min or even 30 min.[30-32] Thus, new devices and methods of high temperature and precision temperature measurement should be exploited for ultra-thick steel plate. Furthermore, smelting and rolling of raw materials, imperfection of mathematical model and solving method are limiting factors for the development of studies on heat transfer during quenching process of ultra-thick steel plate.

In this study, continuous quenching test under various modes of 84~170 mm ultra-thick steel plate was conducted using roller jetting and quenching testing device and multi-channel plate temperature recorder which were especially exploited for ultra-thick steel plate. Temperature dropping curve of typical position for ultra-thick steel plate surface and vertical section was first tested under different medium flow, jetting speed and distance. During the testing process, the jetting water quantity and pressure were dynamically adjusted with the temperature variation of plate wall temperature. The influences of surface heat transfer among jetting stagnation zone, jetting fringe area and lateral flow region to temperature gradient of vertical section were studied under multiple arrays jetting conditions. Furthermore, three dimensional unsteady heat conduction equation of ultra-thick steel plate quenching was constructed and temperature field which was beyond the temperature measuring points was calculated using inverse heat conduction method. The influences of different surface heat transfer conditions to cooling speed were compared and analyzed. Based on nonlinear function, three-dimensional finite element analytical method was used to solve the heat conduction equation in the process of calculation. Heat transfer coefficient distribution function was revealed by the approximative method of serendipity family cubic shape function. And heat flow density distribution function was investigated through optimization methods of Quasi-Newton and BFGS-algorithm. Related achievements will not only provide the theoretical algorithm and experimental data for the researches of quenching cooling speed and cooling uniformity, but also give the effective controlling method to further increase the mechanical and operational properties of ultra-thick steel plate.

2. The Experimental Device and Flow

2.1 Experimental materials

Experimental material is Q345B, high quality low alloy steel after hot rolling supported by NISCO with chemical components (mass fraction %) of 0.18C, 0.24Si, 1.35Mn, ≤ 0.01P, ≤ 0.005S, 0.2Cr, 0.1Mo, 0.2Ni, 0.2Cu, Ceq=0.42. The chose thickness of experimental plate is 84 mm and 170 mm, and the width is 350 mm, the length is 416 mm. After being tested, the critical temperature of steel plate is Ac_1 735°C, Ac_3 863°C, Ar_1 685°C, Ar_3 840°C, M_s 450°C, M_f 150°C. Before each experiment, the surface of steel plate is polished with 360 mesh sandpaper and the actual average roughness of upper surface is 0.3 μm. Handles are welded on steel plate for easy lifting.

The steel plate is punched by YL-100AI desktop drilling machine to install K-type sheathed thermocouple whose type is WRNK-191 and specification is Φ3 mm × 2000 mm × 1000 mm. The diameter of thermocouple wire is 0.8 mm, the material is nickel chromium silicon-nickel silicon magnesium, and the range of temperature measurement is 0~1100°C. The material of protective sleeve of thermocouple is 2520 stainless steel and the wall thickness of protective sleeve is 0.05 mm. After checking, the measuring accuracy of thermocouple is ±1°C within the temperature of 200~1000°C. Fig. 1 shows the locations of temperature measuring points. In our previous studies,[33] the plate surface could be into jet impact heat transfer zone (Z1), nucleate-transition boiling zone (Z2), film boiling zone (Z3) and small liquid accumulation zone (Z4) when jetting and impinging. The locations of temperature measuring points P1, P2 and P3 are set in Z1, Z2 and Z4, respectively. Four temperature measuring points are set in the section of plate which is 2 mm, H/6, H1/3 away from the surface of plate and the center of plate. Therefore, 12 holes are drilled with 3.2 mm diameter and 120 0.5 mm depth. The diameter of the hole is 0.2 mm larger than the diameter of thermocouple for inserting into the bottom of the hole easily. In order to reduce the thermal contact resistance of thermocouple and steel plate, heat-conducting glue for high temperature is filled in the hole before inserting the thermocouple (λ = 9.1 W/(m·K), 927°C maximum working temperature, OCI Americas company).

2.2 Experimental devices

For ultra-thick steel plate, nozzles and rollers arrangements in quenching zone are showed in Fig. 2A and 2B. High pressure cooling section of cooling zone with 360 mm width and 2.8 m effective length is used in the experiments. Eight groups of round jetting nozzles with multi rows and high density are installed in the up and down of the internal devices and the diameter of the nozzles is 3 mm. As the

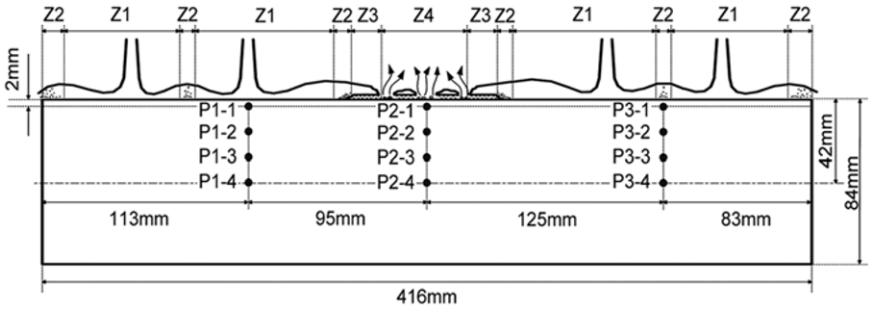

Fig. 1 Locations of temperature measuring points on longitudinal section of steel plate with 84 mm thickness and the corresponding surface heat transfer zone (170 mm-thick steel plate located by thickness ratio)

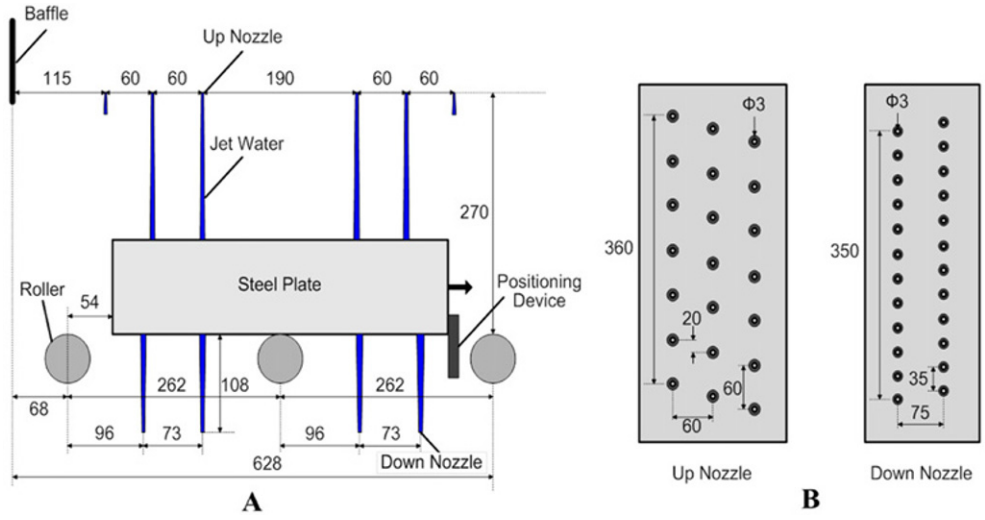

Fig. 2 Parameters of device structures and nozzles for quenching; A: parameters of device structures, B: parameters of quenching nozzles

interactions between water flows strengthen the effect of turbulence, jetting nozzles with multi rows have higher heat transfer efficiency.[28] One group of horizontal rollers having 470 mm roller surface width and 0.5~3.5 m/min adjustable range of roller speed traverse the up and down jetting nozzles. Besides jetting heat transfer, nuclear or membrane heat transfer exists on the upper surface of steel plate for the covering of residual water, while only jetting and radiating heat transfer exist on the down surface for the dropping of residual water. Thus, different heat transferring types of upper and down surfaces cause different structures of jetting nozzles and flow densities. Jetting flow and pressure of every group are continuously adjustable in the high pressure cooling section. The regulating ranges of flow and jetting pressure are 20~200 m^3/h and 0.2~1.2 MPa, respectively. Locating device is designed to ensure quenching in a fixed position and the positional deviation is less than 2 mm after repeated measurements and analysis of statistical results.

Sprinkler system of experimental devices is composed of frequency conversion pump, water supply pipe, controlling valve, jetting nozzle, controlling center and temperature collecting system (Fig. 3). In experiments, cooling water is supplied by frequency conversion pump. Water temperature is tested by temperature sensor. Water jetting pressure is closed-loop controlled by electric controlling valve coordinating with pressure sensor. The amount of jetting water is closed-loop controlled by electromagnetic flow meter coordinating with the frequency of frequency conversion pump. The opening and closing of nozzles is controlled by pneumatic valve and the running speed of plate is closed-loop controlled by roller inverter coordinating with encoder. Controlling center is composed by SIEMENS S7-400 PLC and high performance server which can record the water temperature, pressure, quantity and precisely control the jetting parameters with apparatus. Combining the parameters provided by manufacturers with repeated measurements and analysis of statistical results, the controlling precision of water quantity and pressure is both 1%, the controlling precision of water temperature is 0.5°C and the controlling precision of rolling speed is 0.01 m/min. The real-time temperature of every temperature measuring point is recorded and tested by RAL-31-K type steel plate temperature recorder during the heating and quenching process (Fig. 1). The temperature recorder has 31 temperature recording channels with 0.01°C measuring accuracy and the sampling period is 100 ms. The type of temperature recorder is AD7663ASTZ with internally installed A/D transverter. When testing the temperature, the recorder is connected with thermocouple at one end to collect and record the temperature data using TrendReporter 7 as temperature recording software. Control center is connected with thermocouple at the other end. The changing curve of internal real-time temperature is showed on displayer of

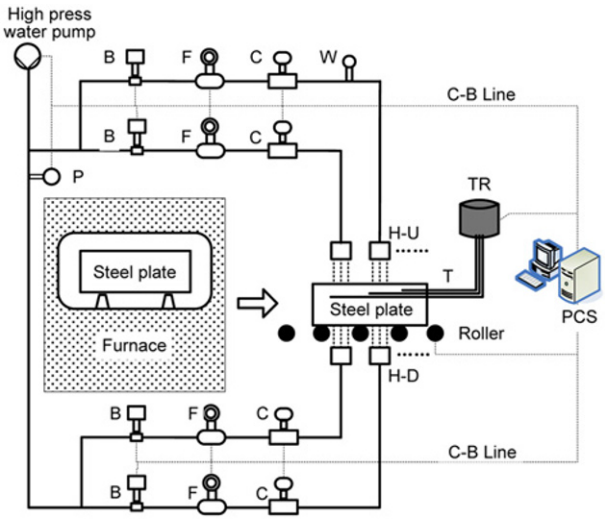

Fig. 3 Configuration of sprinkler system for quenching experimental devices, C: control valve, B: on-off valve, T: thermocouple, W: water temperature gauge, F: flowmeter, P: pressure gauge, TR: temperature tracking recorder, H-U: up jet injection nozzles, H-D: down jet injection nozzles, PCS: control center, C-B Line: control and feedback cable

control center using SIEMENS WINCC as temperature showing and editing software.

2.3 Experimental flow and parameters

Steel plate is heated to 920±2°C in muffle furnace and homogenizing heat preserved for one hour which ensures the uniformity of the section temperature. Before quenching, experimental devices are opened by the setting flow and pressure. The steel plate is lift to inputting rollers by crown block and then goes into quenching zone with 5 m/min speed. In order to study the influences of jetting parameter changing to cooling speed in different quenching temperature dropping stage, four quenching modes are designed for each thickness. In mode I, it has jetting pressure of 1.0 MPa and total water quantity of 100 m^3/h, while in mode II it has jetting pressure of 0.4 MPa and total water quantity of 60 m^3/h. In mode III, 1.0 MPa jetting pressure and 100 m^3/h total water quantity are firstly used to cool down the temperature of plate center near to M_s point and then 0.4 MPa jetting pressure and 60 m^3/h total water quantity are used to cool down the temperature of plate center to room temperature. In mode IV, 0.4 MPa jetting pressure and 60 m^3/h total water quantity are firstly used to cool down the temperature of plate center near to M_s point and then 1.0 MPa jetting pressure and 100 m^3/h total water quantity are used to cool down the temperature of plate center to room temperature. The actual measured temperature of plate center can be directly observed on the display screen of controlling center.

In previous studies, if the total water quantity is 60 m^3/h and 100 m^3/h, the single circular orifice flow will be 0.357 m^3/h and 0.595 m^3/h. The outflow speed of circular orifice v_N will be 14.03 m/s and 23.39 m/s, and the water flow density ρw of corresponding jetting and impacting heat transfer zone (Z1, Fig. 1) will be 3858 L/(m^2min) and 6430 L/(m^2min). The jet impingement moving Re number will be 36410 and 60700, respectively.[3,4] In other studies, if the thickness of steel plate is 84 mm and the jetting length is 186 mm, the jetting and impacting speed v_J will be 14.16 m/s and 23.47 m/s under the above two kinds of total water quantity. If the thickness of steel plate is 170 mm and the jetting length is 100 mm, the jetting and impacting speed v_J will be 14.1 m/s and 23.43 m/s under the above two kinds of total water quantity.[4]

3. Mathematical Model

3.1 Heat transfer equation and formula of inverse heat transfer problem

Basing on the measured temperature drop curve of temperature measuring points and heat conduction differential equation, the quenching temperature field of ultra-thick steel plate is calculated by inverse heat conduction method (IHCM). In this study, three-dimensional unsteady heat conduction equation is set up considering the changing of thermophysical parameter with the temperature as showed in formula 1. As the phase transformation is complex in the quenching process, the phase transformation latent heat is incorporated into the average specific heat of steel plate to construct heat conduction equation with no internal heat source.

$$\frac{\partial T}{\partial \tau}=\frac{\lambda(T)}{c(T)\rho(T)}\left(\frac{\partial^2 T}{\partial x^2}+\frac{\partial^2 T}{\partial y^2}+\frac{\partial^2 T}{\partial z^2}\right) \quad (1)$$

$$0<x<H/2, \quad 0<y<B, \quad 0<z<L, \quad \tau>0$$

Heat conduction equation uses the third boundary condition that the heat transfer coefficient is known. The researching range of IHCM is ~H/2 area of plate surface as showed in Fig. 4. Assuming the lateral heat flux density is 0 (In fact, the lateral heat flux density is less than 0.08% of the upper and lower surfaces.) and there is no heat exchange between the first and second half of thickness (That is completely sy mmetric cooling), initial conditions and boundary conditions can be expressed as:

$$\begin{aligned}
&T(x,y,z)=\Phi, \quad (\tau=0, 0\le x\le H/2, 0\le y\le B, 0\le z\le L)\\
&\overset{g}{q}(y,z,\tau)=h(y,z,\tau)(T_s-T_w), \quad (x=H/2)\\
&\overset{g}{q}(y,z,\tau)=-\lambda(T)\frac{\partial T}{\partial x}=0, \quad (x=0)\\
&\overset{g}{q}(x,z,\tau)=-\lambda(T)\frac{\partial T}{\partial y}=0, \quad (y=0, or, y=B)\\
&\overset{g}{q}(x,y,\tau)=-\lambda(T)\frac{\partial T}{\partial z}=0, \quad (z=0, or, z=L)
\end{aligned} \quad (2)$$

In the above formulas, water temperature variation can be ignored because the test circulating water quantity is high to 60~100 m^3/h (The measured temperature rises 0.3°C). The initial temperature field before quenching can be tested out by measured temperature drop curve.

In quenching process, the distribution of up surface heat flux density can be obtained by solving the minimal value of the objective function *f(pi)* which defines the difference between the measured and calculated values of surface temperature. The expression is:

$$f(p_i)=\frac{1}{N_t N_p}\sum_{m=1}^{N_t}\sum_{n=1}^{N_p}\left(\frac{Te_n^m-T_n^m}{Te_n^m}\right)^2 \quad (3)$$

In the above formula, using finite element method T_n^m can be

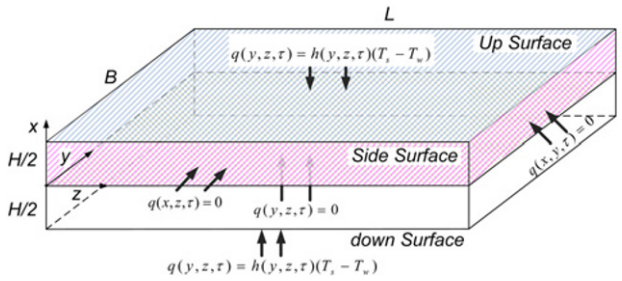

Fig. 4 Coordinates and boundary conditions of three-dimensional conduction problem in steel quenching process

obtained by solving formula (1) as showed below.

Basing on the inverse heat conduction method and measured near surface temperature, HTC distribution of upper surface is approximately calculated using cubic shape functions from serendipity family. The expression is:

$$h(y,z,\tau)=\sum_{i=1}^{12}F_iP_i(\tau) \tag{4}$$

For cubic unit, corner node linear shape function can be expressed as:[35]

$$F_i=\frac{1}{32}(1+\xi_1\xi_{1n})(1+\xi_2\xi_{2n})\left[-10+9\left(\xi_1^2+\xi_2^2\right)\right] \tag{5}$$

Edge node linear shape function can be expressed as:

$$\begin{aligned}F_i&=\frac{9}{32}(1+\xi_2\xi_{2n})\left(1+\xi_1^2\right)(1+9\xi_1\xi_{1n}) \text{ or}\\ F_i&=\frac{9}{32}(1+\xi_1\xi_{1n})\left(1+\xi_2^2\right)(1+9\xi_2\xi_{2n})\end{aligned} \tag{6}$$

In formula (4), $P_i(\tau)$ describes the change of heat transfer coefficient of each element node in a certain time period. The expression is:

$$P_i(\tau)=\sum_{j=1}^{3}W_j(\eta)p_{ij} \tag{7}$$

In the above formula, W_j is parabolic-spline function. p_{ij} is the minimized parameter which can be expressed by node heat transfer coefficient.

In formula (3), the minimal value of the objective function $f(pi)$ can be solved by Quasi-Newton Methods. Using BFGS-algorithm, symmetric positive definite matrices are obtained like Hesse Matrix.[36] As BFGS-algorithm needs to calculate the value of object function and its derivative value in formula (3), formula (3) can be changed into:

$$\frac{\partial f(p_i)}{\partial p_j}=\frac{-2}{N_tN_p}\sum_{m=1}^{N_t}\sum_{n=1}^{N_p}\left(\frac{Te_n^m-T_n^m}{Te_n^m}\right)\frac{\partial T_n^m}{\partial p_j} \tag{8}$$

In order to terminate the problem of unconstrained optimization, the decrease of the objective function value can be controlled by the following principles:

$$\begin{aligned}&\Delta T_{ave}=\sqrt{\frac{1}{N_tN_p}\sum_{m=1}^{N_t}\sum_{n=1}^{N_p}\left(Te_n^m-T_n^m\right)^2}\\ &\Delta T_{ave}^{k+1}-\Delta T_{ave}^{k}<\varepsilon\end{aligned} \tag{9}$$

3.2 The finite element method of heat transfer equation

In order to study the problem of heat transfer, the steel plate showed in Fig. 4 is divided into 8-nod cubic element. Element shape function *Hi* takes Hermitain interpolation polynomial type. Thus, internal temperature field of steel plate can be expressed as:

$$T(x,y,z)=H_iT_i \tag{10}$$

Integral form of formula (1) can be obtained as:[35]

$$A_{ij}T_i+B_{ij}\frac{\partial T_i}{\partial\tau}=C_i \tag{11}$$

For some element, matrices A_{ij}, B_{ij} and vector C_i can be expressed as:

$$A_{ij}=\iiint\lambda(T)\left(\frac{\partial H_i}{\partial x}\frac{\partial H_j}{\partial x}+\frac{\partial H_i}{\partial y}\frac{\partial H_j}{\partial y}+\frac{\partial H_i}{\partial z}\frac{\partial H_j}{\partial z}\right)dV+\iint_{S_e}S_eH_iH_jh(y,z,\tau)dS_e \tag{12}$$

$$B_{ij}=\iiint_V\rho(T)c(T)H_iH_jdV \tag{13}$$

$$C_{ij}=\iint_{S_e}S_eH_ih(y,z,\tau)T_wdS_e\quad i=1,\cdots,F_N;\quad j=1,\cdots,F_N \tag{14}$$

In formula (12)-(14), integration of node temperature and Hermitain interpolation function of derivative can be expressed as:

$$H_i=G_l(\eta_x)G_m(\eta_y)G_n(\eta_z),\quad l,m,n=1,\ldots,4 \tag{15}$$

In the above formula, G_i is cubic spline function. Assuming the temperature linearly changes with time in the minimum time period, formula (11) can be simplified into linear equations by Galerkin integration scheme method. The expression is:

$$\left(\frac{A_m}{3}+\frac{B_m}{2\Delta\tau}\right)T_m=\left(\frac{A_m}{6}+\frac{B_m}{2\Delta\tau}\right)T_m^0-\left(\frac{3\Delta\tau^0+2\Delta\tau}{6\Delta\tau^0}\right)C_V+\frac{\Delta\tau C_V^0}{3\Delta\tau^0} \tag{16}$$

By choosing the weight and shape function, matrices *A*, *B* and vector *C* can be expressed by some formulas.

3.3 Model of thermal physical property parameters

In order to increase the solving precision of three-dimensional heat conduction equation, the changing of specific heat, heat conductivity coefficient and density are measured as the temperature changes. DSC-404-C type Differential Scanning Calorimetry is used for measurement of specific heat (NETZSCH, Germany). LFA-447 type Laser Thermal Conductivity Meter is used for measurement of heat conductivity coefficient (NETZSCH, Germany). In the measurement of density, JmatPro simulation software is firstly used to determine phase composition of steel plate in different temperature. Then, average density of steel plate is calculated according to each phase. The thermal physical parameters fitting summation formula is obtained as follows:

$$\begin{cases}c(T)=462.32+0.3188T-1.61\times10^{-4}T^2+7.866\times10^{-7}T^3, & T\in[25,675]\\ c(T)=5526.3+9.44T, & T\in(675,725]\\ c(T)=21751.05-47.833T+0.0271T^2, & T\in(725,875]\\ c(T)=542.92+0.1086T, & T\in(875,1325].\end{cases} \tag{17}$$

$$\begin{cases}\lambda(T)=45.11-0.0125T-0.000017T^2, & T\in(0,825];\\ \lambda(T)=27.24-\dfrac{5.657}{1+e^{(T-1110.7)/125.22}}, & T\in(825,1325].\end{cases} \tag{18}$$

$$\begin{aligned}
&\rho(T) = 7815.86 - 0.2139T - 1.2494\times10^{-4}T^2, && T \in [0,500];\\
&\rho(T) = 9516.357 - 7.4562T + 0.00956T^2 + -4\times10^{-6}T^3, && T \in (500,800];\\
&\rho(T) = 7555.75 + 0.485T - 5\times10^{-4}T^2, && T \in [0,500].
\end{aligned} \quad (19)$$

4. Results of Experiments and Calculation and Analysis of Errors

Based on the measured near-surface temperature of steel plate, surface heat-transfer coefficient is calculated by inverse heat transfer method. And then temperature drop curve of temperature measuring points is calculated by solving heat transfer equation using finite element method. Fig. 5 shows the comparison of calculated and measured values of temperature drop curve at temperature measuring points P1-1, P1-2, P1-3 and P1-4 according to mode III in quenching process. The result shows good agreement and the deviation is less than 4%. Calculating conditions of quenching temperature drop curve for 84 mm-thick steel plate are as follows. Starting cooling temperatures of near-surface and center are 825°C and 871°C, respectively. It is firstly quenched with 100 m^3/h water quantity and 1.0MPa water pressure for 104 s whose average surface heat transfer coefficient is 22000 W $(m^2\,°C)^{-1}$. Then, it is quenched with 60 m^3/h water quantity and 0.4 MPa water pressure for 183 s whose average surface heat transfer coefficient is 6000 W $(m^{2o}C)^{-1}$. The temperature of water is 11.5°C. Calculating conditions of quenching temperature drop curve for 170 mm-thick steel plate are as follows. Starting cooling temperatures of near-surface and center are 789°C and 877°C, respectively. It is firstly quenched with 100 m^3/h water quantity and 1.0 MPa water pressure for 335 s whose average surface heat transfer coefficient is 25000 W $(m^{2o}C)^{-1}$. Then, it is quenched with 60 m^3/h water quantity and 0.4 MPa water pressure for 412 s whose average surface heat transfer coefficient is 6500 W $(m^{2o}C)^{-1}$. The temperature of water is 12.7°C. After analysis, the reasons of deviation are summarized for two aspects, measurement and model calculation. Combining with the all experiments, measuring deviations mainly contain thermocouple temperature measurement deviation (± 1°C), jetting parameters measurement deviation (± 1%), and steel plate location deviation (± 2 mm, determined by controlling precision of rolling speed). Model calculation deviation mainly considers the following several aspects. As using fitting function form, the deviation between calculated and measured values of thermophysical parameter is 0.5%. Heat transfer equation is solved by finite element method based on interpolating polynomial shape function. Heat transfer coefficient is solved by finite element method based on serendipity family cubic shape function. The method of discrete solution will make 1% deviation. Phase transformation latent heat in quenching process is changed into average specific heat to calculate temperature field. However, phase transformation of steel plate does not occur at the same time which causes 1% deviation on the calculation of average specific heat. Further analysis shows that calculated temperature drop curve has obvious turning point while measured temperature drop curve is quite gentle when the water pressure drops from 1.0 MPa to 0.4 MPa. This is because the surface heat transfer coefficient instantly changes with the dropping of water pressure in calculating which causes the fluctuation of curve, while the surface heat transfer coefficient continuously changes with the dropping of water pressure in measuring. Calculating

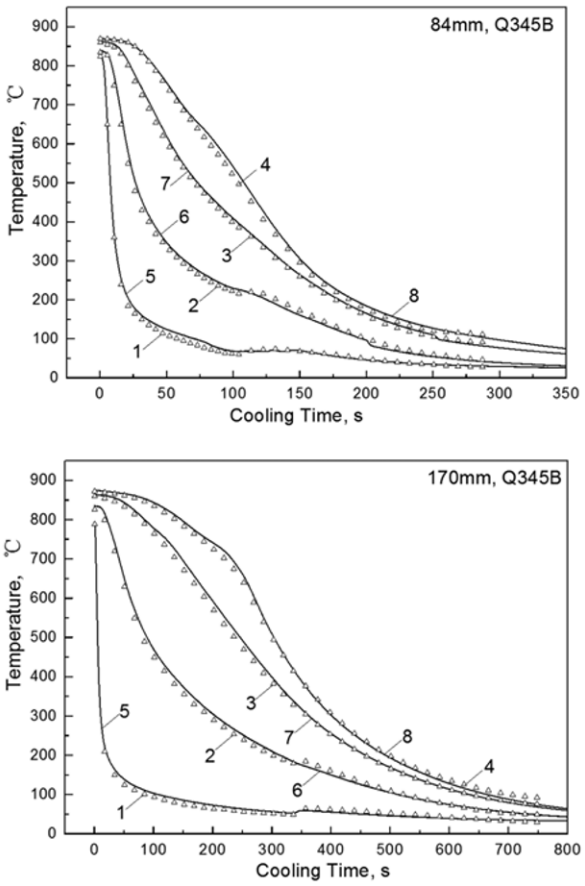

Fig. 5 Comparison of calculated and measured values of temperature drop curve in quenching process. 1: surface calculated curve (P1-1); 2: *H*/6 calculated curve (P1-2); 3: *H*/3 calculated curve (P1-3); 4: *H*/2 calculated curve (P1-4); 5: surface measured curve (P1-1); 6: *H*/6 measured curve (P1-2); 7: *H*/3 measured curve (P1-3); 8: *H*/2 measured curve (P1-4)

deviation in transient change of heat transfer coefficient is about 1%.

In calculating process of temperature drop curve, the used surface heat transfer coefficient can be reverse calculated based on the measured surface temperature curve of steel plate. As the number of surface temperature measuring points is limited, surface heat transfer coefficient will be closer to the measured value when being closer to the actual temperature measuring point which makes the calculation of temperature field more accurately. As the region of vertical section near temperature measuring point is the scope of this research, the existing calculation accuracy can satisfy the further analysis.

5. Analysis and Discussion

5.1 The influence of quenching mode to temperature drop curve

Fig. 6 shows the temperature drop curves of ultra-thick steel plate under quenching modes I-IV. The cost time making the center temperature of 84 mm-thick steel plate drop below 100°C under four quenching modes is 262 s, 589 s, 297 s and 462 s, respectively, which differs 327 s for different quenching modes (Fig. 6A~D). In the same

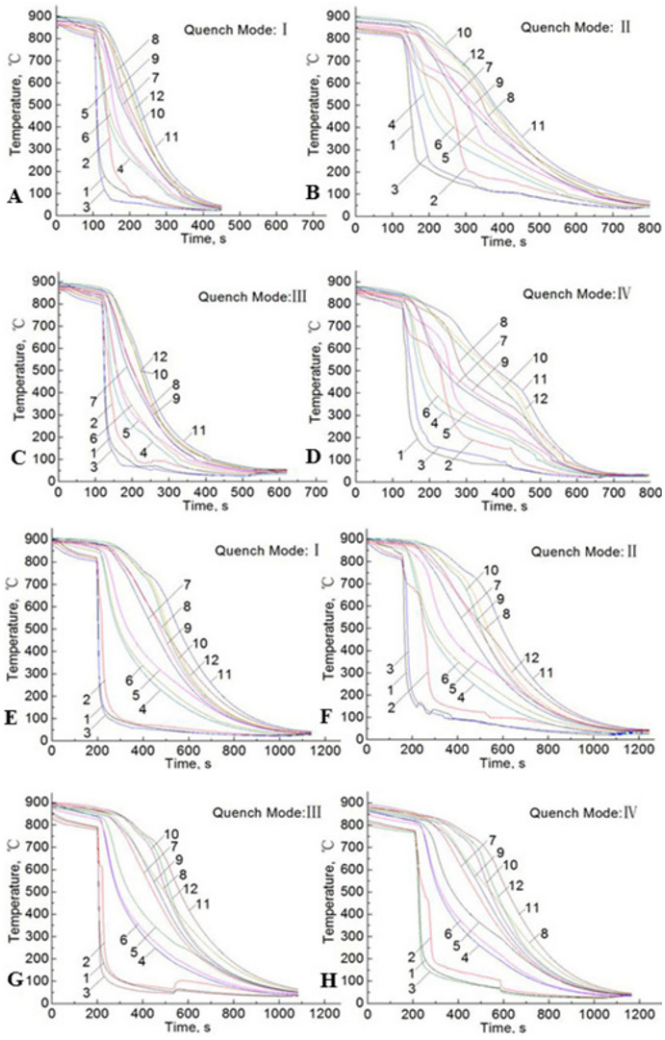

Fig. 6 Temperature drop curves of ultra-thick steel plate in quenching process, A-D are quenching modes I-IV with 84 mm thickness, E-H are quenching modes I-IV with 170 mm thickness. The 1-12 curves are corresponding with the temperature measuring points P1-1, P2-1, P3-1, P1-2, P2-2, P3-2, P1-3, P2-3, P3-3, P1-4, P2-4 and P3-4 in Fig. 1

conditions, the cost time is 688 s, 804 s, 729 s and 743 s, respectively, for 170 mm-thick steel plate which only differs 116 s for different quenching modes (Fig. 6E~H). Therefore, the influences of the changing of quenching modes to temperature dropping of steel plate section become weak with the increasing of thickness. Comparative analysis of curves in Fig. 6A~D shows that the cooling speed with large water pressure and current (mode I and III) in H/6~H/2 region is significantly faster than that with small water pressure and current (mode II and IV) for 84 mm-thick steel plate within high temperature period. The uniformity of temperature is better for the increasing of center-surface heat flux density when the surface heat transfer coefficient increases and temperature gradient enlarges. Further comparative analysis of two curves in Fig. 6A and C shows that the near-center temperature drop does not slow down significantly which has little difference with temperature drop curve in mode I, because the greater center-surface temperature gradient has been formed although small water pressure and current are used for quenching after the center temperature drop

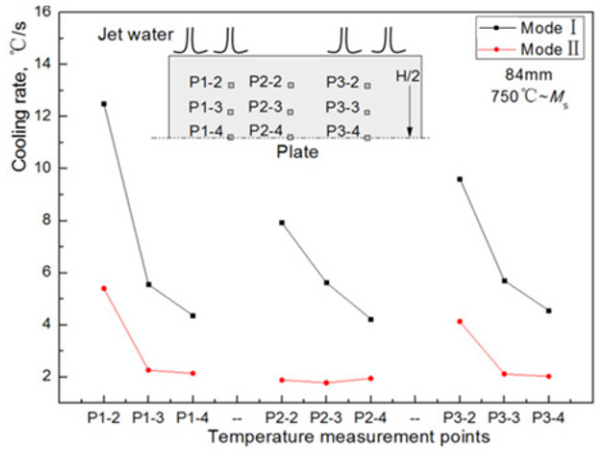

Fig. 7 Distribution of cooling speed in quenching process within high temperature period for 84 mm-thick steel plate

below M_s point in mode III. Simultaneous analysis of two curves in Figs. 6B and 6D shows that when small water pressure and current are first used, the surface heat transfer coefficient is relatively small and greater temperature gradient forms in surface~H/6 region without penetrating to center which causes the temperature drop to slow down in H/6~H/2 region. When the center temperature slowly drops below M_s point, the temperature drop in surface~H/6 region increases rapidly using large water pressure and current (Fig. 6D, mode III) which causes temperature gradient in H/6~H/2 region enlarges and temperature drops obviously. Thus, the temperature drop for 84 mm-thick steel plate is closely related with the temperature gradient while the temperature gradient is greatly influenced by quenching modes (I-IV). Comparing the curves in Fig. 6E-F, the changing of quenching modes only has great influence to temperature gradient in surface~H/6 region with the increasing of plate thickness while the temperature drop in H/6~H/2 region is mainly related with the inherent heat transfer ability such as thermal physical parameter (formula 1). Therefore, temperature drop curve in quenching process does not change obviously in different quenching mode (I-IV) for 170 mm-thick steel plate.

5.2 Distributing regularities and influencing factors of cooling speed in quenching process for 84 mm-thick steel plate

5.2.1 Cooling speed of quenching within high temperature period (750°C~Ms) for 84 mm-thick steel plate

Fig. 7 shows the distribution of cooling speed in 750°C~M_s region for 84 mm-thick steel plate. As the quenching parameters of quenching mode I and III, mode II and IV are the same in this temperature period, only cooling speeds for quenching mode I and II are listed in the figure. As the surface cooling speeds in both modes can satisfy the requirements of quenching, surface cooling speeds are not showed in Fig. 7. Comparing with mode II, mode I increases the cooling speed by more than three times, especially the average center cooling speed from 2.04°C/s to 4.4°C/s. Comparing Fig. 8 with Fig. 9, cooling speed in surface~H/6 region is approximately proportional to average heat transfer coefficient of each surface heat transfer zone. P1-1 is in Z1 zone of Fig. 1 and the cooling water jet directly on plate surface. The average surface heat transfer coefficient reaches to 21200 W $(m^{2o}C)^{-1}$ and the corresponding

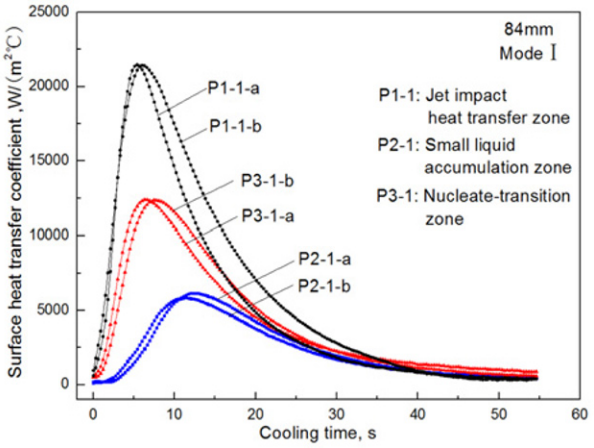

Fig. 8 The average heat transfer coefficient in different heat transfer zones of steel plate

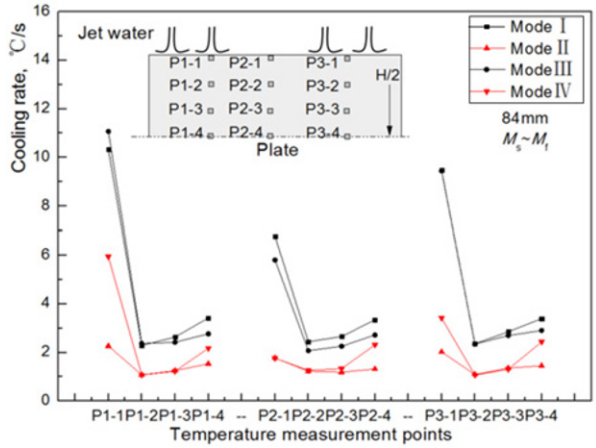

Fig. 9 Distribution of cooling speed in quenching process within middle temperature period for 84 mm-thick steel plate

cooling speed for P1-2 is 12.9°C/s. P3-1 is in Z2 zone of Fig. 1. According to the previous studies,[37] the cooling water laterally flows along the wall. The upper layer is the turbulence main flow zone while the down layer is the nucleate-transition boiling zone. The average surface heat transfer coefficient is 13200 W $(m^{2o}C)^{-1}$ and the corresponding cooling speed for P3-2 is 9.2°C/s. P2-1 is in Z4 zone of Fig. 1. Small droplets gather on the plate surface which forms the heat transfer zone combining discontinuous film boiling with radiant heat transfer. The average surface heat transfer coefficient is only 7000 W $(m^{2o}C)^{-1}$ and the corresponding cooling speed for P3-2 is only 7.7°C/s. In the same quenching mode, the influences of distribution of surface heat transfer zones to cooling speeds at *H*/3 and *H*/2 locations decrease and the average cooling speeds are about 5.6°C/s and 4.3°C/s. In mode II, the difference of surface heat transfer coefficient also impacts the cooling speeds at 1/6*H* location but not significantly like mode I. The cooling speeds at *H*/3 and *H*/2 locations are almost the same, about 2.1°C/s, which indicates the center cooling speed in mode II has no relationship with the distribution of surface heat transfer zones. It is worth noting that the corresponding cooling speed of small liquid accumulation zone (P2-1 location) in mode II has no relationship with the distances to surface. The cooling speeds of P2-2, P2-3 and P2-4 locations are all about 1.85°C/s which indicates the relative low heat transfer coefficient of this zone reduces the temperature gradient forming triangle zone with high temperature when being quenched with small water pressure and current. The appearance of this triangle zone reduces the cooling uniformity of plate center.

5.2.2 Cooling speed of quenching within middle temperature period (Ms~Mf) for 84 mm-thick steel plate

Fig. 9 shows the distribution of cooling speed in M_s~M_f period for 84 mm-thick steel plate. Being similar to Fig. 7, the cooling speed with large water pressure and current (mode I and III) is faster than that with small water pressure and current (mode II and IV), and the heat transfer ability in surface~*H*/6 region is approximately proportional to cooling speed. For example, in mode I, the cooling speeds of jet impact zone (P1-1), nucleate-transition boiling zone (P1-3) and small liquid accumulation zone (P1-2) decrease systematically which are 10.3°C/s, 9.46°C/s and 6.77°C/s, respectively. Being different with Fig. 7, the cooling speed in *H*/6~*H*/2 region does not decrease but rises with the increase of distance to surface in mode I, III and IV. P1-2, P2-2 and P3-2 are the minimum points of cooling speed in the same heat transfer zone which decreases about 50% than center cooling speed. However, in mode II, the cooling speeds of corresponding points in the same heat transfer zone are essentially equal. This phenomenon is related with the distribution of section temperature gradient after quenching.

The temperature of near surface drops quickly when quenching within high temperature period. Temperature gradient in surface~*H*/6 region increases rapidly causing obvious temperature dropping in this region. However, in *H*/6~*H*/2 region, temperature dropping is comparatively slow and temperature gradient is relatively small because of the plate transfer ability. With the end of quenching within high temperature period, continuous middle temperature period (M_s~M_f) comes and the temperature of plate in surface~*H*/6 region is relatively low with limited space for temperature dropping. In *H*/6~*H*/2 region, heat continuously transfers to surface with the gradual increase of temperature gradient which makes the cooling speed increase in the same quenching time.

Further analysis shows that the influence of distribution of heat transfer zone to cooling speed at *H*/6 and *H*/2 locations is small, such as the difference of cooling speed at P1-2 and P1-4, P2-2 and P2-4, P3-2 and P3-4 locations is all about 1.4?/s in modes I, II and III. However, the difference of cooling speed at *H*/6 and *H*/2 locations increases with reducing of surface heat transfer ability in mode IV. For example, the difference of cooling speed at P1-2 and P1-4 locations is only 0.4?/s, but the difference of cooling speed at P2-2 and P2-4 locations increases to 1.2°C/s. In mode IV, small water pressure and current is used for quenching within high temperature period while large water pressure and current is employed within middle temperature period. The change of surface heat transfer zone improves the surface heat transfer ability of small liquid accumulation zone. Relative great temperature gradient after being quenched within high temperature period in *H*/6~*H*/2 region significantly increases the amount of heat conduction at P2-2, P2-3 and P2-4 locations. All of these cause the remarkable increase of cooling speed. Thus, the change of surface heat transfer zone and temperature

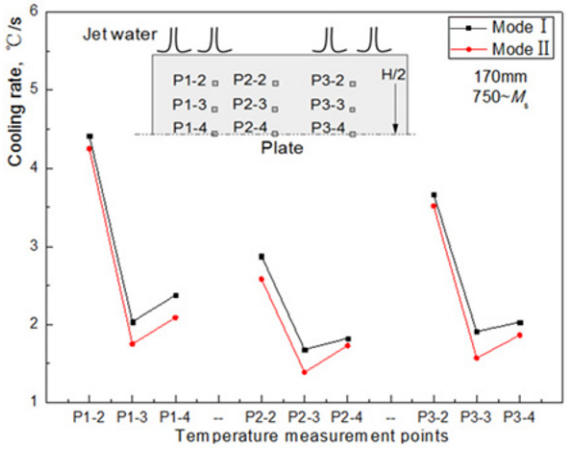

Fig. 10 Distribution of cooling speed in quenching process within high temperature period for 170 mm-thick steel plate

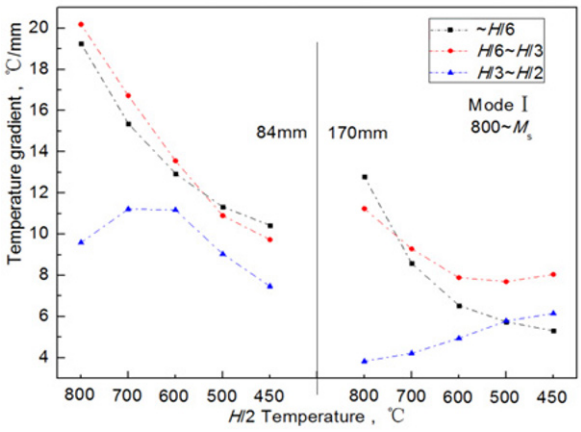

Fig. 11 Gradient comparison of temperature in quenching process

genetic effect after being quenched within high temperature period collectively impact the distribution of cooling speed of vertical section within middle temperature period. The former mainly influences the cooling speed in surface~*H*/6 region and the latter effects that in *H*/6~*H*/2 region.

5.3 Distributing regularities and influencing factors of cooling speed in quenching process for 170 mm-thick steel plate

5.3.1 Cooling speed of quenching within high temperature period (750°C~Ms) for 170 mm-thick steel plate

Fig. 10 shows the distribution of cooling speed in 750°C~M_s period for 170 mm-thick steel plate. The cooling speeds of vertical section under mode I and mode II are compared and analyzed like Fig. 8. Under both modes, cooling speed of 170 mm-thick steel plate is approximately proportional to surface heat transfer ability in surface~*H*/6 region, while the influence of surface heat transfer ability to cooling speed is unconspicuous in *H*/6~*H*/2 region. Under mode I, the cooling speeds of P1-3, P2-3 and P3-3 locations only differ 0.33°C/s, and under mode II, the cooling speeds of three locations only differ 0.32°C/s. This rule is consistent with that of 84 mm-thick steel plate. Further comparison shows that the difference of cooling speed of vertical section for 170 mm-thick steel plate is much less than the difference for 84 mm-thick steel plate because of the different quenching mode. For example, the difference of cooling speed for 84 mm-thick steel plate at P1-3 location is 3.29°C/s, while the difference for 170 mm-thick steel plate reduces to 0.29°C/s shrinking more than 10 times. This rule is more obvious at *H*/6 location. Being different with that of 84 mm-thick steel plate, the quenching cooling speed within high temperature period increases with the increase of distance to surface for *H*/3~*H*/2 range of 170 mm-thick steel plate which makes the *H*/3 location (not *H*/2 location) become the minimum point of cooling speed of vertical section. The above rule is related with the changing of temperature field in surface~*H*/6 range as the changing of surface heat transfer condition and the weakening influence of cooling speed in *H*/3~*H*/2 range. Comparing with the temperature gradient in surface-1/2*H* range within 750°C~M_s temperature period for 84 mm-thick steel plate, the temperature gradient especially in surface~*H*/6 range for 170 mm-thick steel plate decreases 50% in the same conditions as showed in Fig. 13. Moreover, with the decreasing of temperature, the temperature gradient increases gradually in *H*/6~*H*/3 and *H*/3~*H*/2 ranges. In Fourier heat transfer law, the increasing of heat flow density causes the cooling speed not decrease but rise. Therefore, the influence of the changing of surface heat transfer condition to cooling speed becomes weaken with the increasing of plate thickness. Temperature gradient becomes the major factor to affect the cooling speed besides the physical parameter of steel plate.

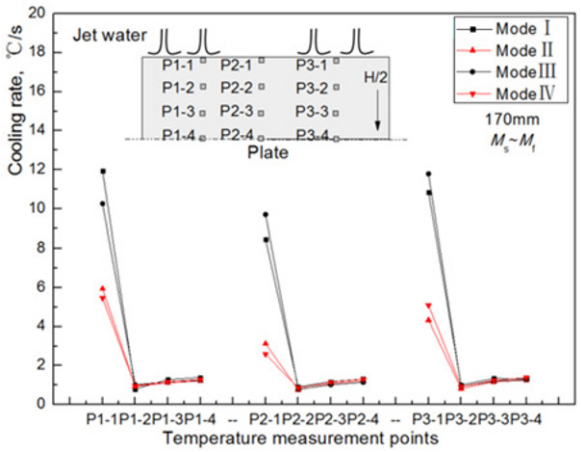

Fig. 12 Distribution of cooling speed in quenching process within middle temperature period for 170 mm-thick steel plate

5.3.2 Cooling speed of quenching within middle temperature period (750°C Ms~Mf) for 170 mm-thick steel plate

Fig. 12 shows the distribution of cooling speed within M_s~M_f temperature period for 170 mm-thick steel plate. The cooling speeds of quenching in the other zones are basically the same except those in the surface to *H*/6 region which are not influenced by quenching modes (mode I-IV) and surface heat transfer zones (jet impact zone, nucleate-transition boiling zone and small liquid accumulation zone) with the average deviation of 0.15°C/s. In the surface to *H*/6 region, the cooling speed of quenching with large water pressure and current (mode I and III) is the double of that with small water pressure and current (mode

II and IV) and the cooling speed is approximately proportional to the average heat transfer coefficient of each heat transfer zone. The Figs. 9 and 10 show that the cooling speed of quenching in M_s~M_f region is simultaneously with temperature genetic effect in 750°C~M_s region after being quenched and the gradient distribution of temperature in M_s~M_f region. With the increasing of thickness, temperature field tends to be uniform after being quenched in 750°C~M_s region under different quenching mode which is hardly influenced by surface heat transfer. Furthermore, the gradient distribution of temperature in M_s~M_f region is also hardly influenced by surface heat transfer. Thus, the cooling speeds of quenching within the range of 1.17~1.32°C/s are basically the same in M_s~M_f region with H/6~H/2 thickness for 170 mm steel plate.

6. Conclusion

Using the newly developed array jet impinging and quenching test apparatus and multi-channel temperature recorder, the corresponding temperature drop curve of vertical section of typical surface heat transfer region was tested for Q345B steel plate with 84 mm and 170 mm thickness under four quenching modes (I-IV). Based on heat anti transfer method, heat conduction model, surface heat transfer coefficient model and thermal physical parameter model are built up and then solved using the methods of finite element, numerical analysis and so on. The calculating deviation of models is less than 4%.

Comparative analysis indicates that the cooling speed of ultra-thick steel plate is also related with the distribution of surface heat transfer coefficient, temperature genetic effect and gradient distribution of temperature besides the inherent thermal physical parameter. When the steel plate has relatively small thickness like 84 mm, heat exchange capabilities of surface jetting and impacting zone, nucleate and transition boiling zone, small liquid residential zone are approximately proportional to the corresponding cooling speed which can form high temperature triangle zone. As the thickness of steel plate increases to 170 mm, the influences of surface heat exchange capabilities to cooling speed, especially cooling speed of near center, become weaken which makes deviation of cooling speed drop to 0.3°C/s. The influences of temperature genetic effect and gradient distribution of temperature to cooling speed are strengthened which makes the cooling speed of H/6~H/2 thickness region not drop but rise with the increasing distance to surface. Thus, H/6~H/3 region has the minimum cooling speed and the average range of cooling speed is 1.0~1.8°C/s in different quenching modes. After comparison, the optimal quenching mode for 84 mm-thick steel plate is mode III considering water saving, and the optimal quenching mode for 170 mm-thick steel plate is mode II.

These results contribute to increasing the cooling speed and formulating better quenching strategy, and further have the reference value for optimization of heat treatment microstructure properties and minimization of quenching.

ACKNOWLEDGEMENT

This study was financially supported by grants from the National Natural Science Foundation of China (51104045), and the basic scientific research funding of ministry of education (N130407006).

REFERENCES

1. Wang, H., Yu, W., and Cai, Q., "Experimental Study of Heat Transfer Coefficient on Hot Steel Plate during Water Jet Impingement Cooling," Journal of Materials Processing Technology, Vol. 212, No. 9, pp. 1825-1831, 2012.
2. Li, X., Wang, M., and Du, F., "A Coupling Thermal Mechanical and Microstructural Fe Model for Hot Strip Continuous Rolling Process and Verification," Materials Science and Engineering: A, Vol. 408, No. 1, pp. 33-41, 2005.
3. Cao, Z.-Q., Bao, Y.-P., Xia, Z.-H., Luo, D., Guo, A.-M., and Wu, K.-M., "Toughening Mechanisms of a High-Strength Acicular Ferrite Steel Heavy Plate," International Journal of Minerals, Metallurgy, and Materials, Vol. 17, No. 5, pp. 567-572, 2010.
4. Karwa, N., Gambaryan-Roisman, T., Stephan, P., and Tropea, C., "Experimental Investigation of Circular Free-Surface Jet Impingement Quenching: Transient Hydrodynamics and Heat Transfer," Experimental Thermal and Fluid Science, Vol. 35, No. 7, pp. 1435-1443, 2011.
5. Karwa, N., Gambaryan-Roisman, T., Stephan, P., and Tropea, C., "Experimental Investigation of Circular Free-Surface Jet Impingement Quenching: Transient Hydrodynamics and Heat Transfer," Experimental Thermal and Fluid Science, Vol. 35, No. 7, pp. 1435-1443, 2011.
6. Liu, Z.-H., Tong, T.-F., and Qiu, Y.-H., "Critical Heat Flux of Steady Boiling for Subcooled Water Jet Impingement on the Flat Stagnation Zone," Journal of Heat Transfer, Vol. 126, No. 2, pp. 179-183, 2004.
7. Wang, L., Sundén, B., Borg, A., and Abrahamsson, H., "Heat Transfer Characteristics of an Impinging Jet in Crossflow," Journal of Heat Transfer, Vol. 133, No. 12, Paper No. 122202, 2011.
8. Lee, P., Choi, H., and Lee, S., "The Effect of Nozzle Height on Cooling Heat Transfer from a Hot Steel Plate by an Impinging Liquid Jet," ISIJ International, Vol. 44, No. 4, pp. 704-709, 2004.
9. Liu, Z. D., Fraser, D., and Samarasekera, I. V., "Experimental Study and Calculation of Boiling Heat Transfer on Steel Plates during Runout Table Operation," Canadian Metallurgical Quarterly, Vol. 41, No. 1, pp. 63-74, 2002.
10. Heo, M.-W., Lee, K.-D., and Kim, K.-Y., "Optimization of an Inclined Elliptic Impinging Jet with Cross Flow for Enhancing Heat Transfer," Heat and Mass Transfer, Vol. 47, No. 6, pp. 731-742, 2011.
11. Lindeman, B. A., Anderson, J. M., and Shedd, T. A., "Predictive Model For Heat Transfer Performance of Oblique and Normally Impinging Jet Arrays," International Journal of Heat and Mass Transfer, Vol. 62, pp. 612-619, 2013.
12. Ochi, T., Nakanishi, S., and Kaji, M., "Multi-phase and Heat Transfer III. Part A: Fundamentals-Cooling of a Hot Plate with an

Impinging Circular Water Jet," Elsevier Science, Publishers B.V., Amsterdam, pp. 8-15, 1984.

13. Wolf, D. H., "Turbulent Development in a Free-Surface Jet and Impingement Boiling Heat Transfer," Ph.D. Thesis, Department of Mechanical Engineering, Purdue University, 1993.
14. Robidou, H., Auracher, H., Gardin, P., and Lebouché, M., "Controlled Cooling of a Hot Plate with a Water Jet," Experimental Thermal and Fluid Science, Vol. 26, No. 2, pp. 123-129, 2002.
15. Ishigai, S., Nakanishi, S., and Ochi, T., "Boiling Heat Transfer for a Plane Water Jet Impinging on a Hot Surface," Proc. of the 6th International Heat Transfer Conference, Vol. 1, pp. 445-450, 1978.
16. Gradeck, M., Kouachi, A., Lebouché, M., Volle, F., Maillet, D., and Borean, J., "Boiling Curves in Relation to Quenching of a High Temperature Moving Surface with Liquid Jet Impingement," International Journal of Heat and Mass Transfer, Vol. 52, No. 5, pp. 1094-1104, 2009.
17. Liu, Z.-H. and Wang, J., "Study on Film Boiling Heat Transfer for Water Jet Impinging on High Temperature Flat Plate," International Journal of Heat and Mass Transfer, Vol. 44, No. 13, pp. 2475-2481, 2001.
18. Miyasaka, Y., Inada, S., and Owase, Y., "Critical Heat Flux and Subcooled Nucleate Boiling in Transient Region between a Two-Dimensional Water Jet and a Heated Surface," Journal of Chemical Engineering of Japan, Vol. 13, No. 1, pp. 29-35, 1980.
19. Ciofalo, M., Di Piazza, I., and Brucato, V., "Investigation of the Cooling of Hot Walls by Liquid Water Sprays," International Journal of Heat and Mass Transfer, Vol. 42, No. 7, pp. 1157-1175, 1999.
20. Buczek, A. and Telejko, T., "Inverse Determination of Boundary Conditions during Boiling Water Heat Transfer in Quenching Operation," Journal of Materials Processing Technology, Vols. 155-156, pp. 1324-1329, 2004.
21. Buczek, A. and Telejko, T., "Investigation of Heat Transfer Coefficient during Quenching in Various Cooling Agents," International Journal of Heat and Fluid Flow, Vol. 44, pp. 358-364, 2013.
22. Beck, J. V., Blackwell, B., and Haji-Sheikh, A., "Comparison of Some Inverse Heat Conduction Methods using Experimental Data," International Journal of Heat and Mass Transfer, Vol. 39, No. 17, pp. 3649-3657, 1996.
23. Jarny, Y., "Determination of Heat Sources and Heat Transfer Coefficient for Two-Dimensional Heat Flow-Numerical and Experimental Study," International Journal of Heat and Mass Transfer, Vol. 44, No. 7, pp. 1309-1322, 2001.
24. Su, J. and Hewitt, G. F., "Inverse Heat Conduction Problem of Estimating Time-Varying Heat Transfer Coefficient," Numerical Heat Transfer, Part A: Applications, Vol. 45, No. 8, pp. 777-789, 2004.
25. Huang, C.-H. and Wang, S.-P., "A Three-Dimensional Inverse Heat Conduction Problem in Estimating Surface Heat Flux by Conjugate Gradient Method," International Journal of Heat and Mass Transfer, Vol. 42, No. 18, pp. 3387-3403, 1999.
26. Kim, S. K., Lee, J.-S., and Lee, W. I., "A Solution Method for a Nonlinear Three-Dimensional Inverse Heat Conduction Problem using the Sequential Gradient Method Combined with Cubic-Spline Function Specification," Numerical Heat Transfer: Part B: Fundamentals, Vol. 43, No. 1, pp. 43-61, 2003.
27. Zhou, J., Zhang, Y., Chen, J., and Feng, Z., "Inverse Estimation of Front Surface Temperature of a Plate with Laser Heating and Convection-Radiation Cooling," International Journal of Thermal Sciences, Vol. 52, pp. 22-30, 2012.
28. Malinowski, Z., Telejko, T., Hadała, B., Cebo-Rudnicka, A., and Szajding, A., "Dedicated Three Dimensional Numerical Models for the Inverse Determination of the Heat Flux and Heat Transfer Coefficient Distributions Over the Metal Plate Surface Cooled By Water," International Journal of Heat and Mass Transfer, Vol. 75, pp. 347-361, 2014.
29. Edalatpour, S., Saboonchi, A., and Hassanpour, S., "Effect of Phase Transformation Latent Heat on Prediction Accuracy of Strip Laminar Cooling," Journal of Materials Processing Technology, Vol. 211, No. 11, pp. 1776-1782, 2011.
30. Abbasi, B., Kim, J., and Marshall, A., "Dynamic Pressure based Prediction of Spray Cooling Heat Transfer Coefficients," International Journal of Multiphase Flow, Vol. 36, No. 6, pp. 491-502, 2010.
31. Slayzak, S. J., Viskanta, R., and Incropera, F. P., "Effects of Interaction Between Adjacent Free Surface Planar Jets on Local Heat Transfer from the Impingement Surface," International Journal of Heat and Mass Transfer, Vol. 37, No. 2, pp. 269-282, 1994.
32. Freund, S., Pautsch, A. G., Shedd, T. A., and Kabelac, S., "Local Heat Transfer Coefficients in Spray Cooling Systems Measured with Temperature Oscillation IR Thermography," International Journal of Heat and Mass Transfer, Vol. 50, No. 9, pp. 1953-1962, 2007.
33. Fu, T. L., Wang, Z. D., Li, Y., Li, J. D., and Wang, G. D., "The Influential Factor Studies on the Cooling Rate of Roller Quenching for Ultra Heavy Plate," Applied Thermal Engineering, Vol. 70, No. 1, pp. 800-807, 2014.
34. Polat, S., Huang, B., Mujumdar, A. S., and Douglas, W., "Numerical Flow and Heat Transfer under Impinging Jets: A Review," Annual Review of Heat Transfer, Vol. 2, No. 2, pp. 157-197, 1989.
35. Zienkiewicz, O. C. and Taylor, R. L., "The Finite Element Method: Solid Mechanics," Butterworth-Heinemann, 5th Ed., pp. 26-32, 2000.
36. Andrei, N., "Accelerated Scaled Memoryless BFGS Preconditioned Conjugate Gradient Algorithm for Unconstrained Optimization," European Journal of Operational Research, Vol. 204, No. 3, pp. 410-420, 2010.
37. Timm, W., Weinzierl, K., and Leipertz, A., "Heat Transfer in Subcooled Jet Impingement Boiling at High Wall Temperatures," International Journal of Heat and Mass Transfer, Vol. 46, No. 8, pp. 1385-1393, 2003.